



Nanodomains can persist at physiologic temperature in plasma membrane vesicles and be modulated by altering cell lipids^S

Guangtao Li,¹ Qing Wang,¹ Shinako Kakuda, and Erwin London²

Department of Biochemistry and Cell Biology, Stony Brook University, Stony Brook, NY 11794-5215

ORCID ID: 0000-0002-1295-0113 (E.L.)

Abstract The formation and properties of liquid-ordered (Lo) lipid domains (rafts) in the plasma membrane are still poorly understood. This limits our ability to manipulate ordered lipid domain-dependent biological functions. Giant plasma membrane vesicles (GPMVs) undergo large-scale phase separations into coexisting Lo and liquid-disordered lipid domains. However, large-scale phase separation in GPMVs detected by light microscopy is observed only at low temperatures. Comparing Förster resonance energy transfer-detected versus light microscopy-detected domain formation, we found that nanodomains, domains of nanometer size, persist at temperatures up to 20°C higher than large-scale phases, up to physiologic temperature. The persistence of nanodomains at higher temperatures is consistent with previously reported theoretical calculations. To investigate the sensitivity of nanodomains to lipid composition, GPMVs were prepared from mammalian cells in which sterol, phospholipid, or sphingolipid composition in the plasma membrane outer leaflet had been altered by cyclodextrin-catalyzed lipid exchange. Lipid substitutions that stabilize or destabilize ordered domain formation in artificial lipid vesicles had a similar effect on the thermal stability of nanodomains and large-scale phase separation in GPMVs, with nanodomains persisting at higher temperatures than large-scale phases for a wide range of lipid compositions. This indicates that it is likely that plasma membrane nanodomains can form under physiologic conditions more readily than large-scale phase separation. We also conclude that membrane lipid substitutions carried out in intact cells are able to modulate the propensity of plasma membranes to form ordered domains. **■** This implies lipid substitutions can be used to alter biological processes dependent upon ordered domains.—Li, G., Q. Wang, S. Kakuda, and E. London. Nanodomains can persist at physiologic temperature in plasma membrane vesicles and be modulated by altering cell lipids. *J. Lipid Res.* 2020. 61: 758–766.

Supplementary key words giant vesicles • phase separation • lipid substitution

This work was supported by National Institutes of Health Grant GM122493. The content is solely the responsibility of the authors and does not necessarily represent the official views of the National Institutes of Health. The authors declare that they have no conflicts of interest with the contents of this article.

Manuscript received 3 December 2019 and in revised form 6 January 2020.

*Published, JLR Papers in Press, January 21, 2020
DOI <https://doi.org/10.1194/jlr.RA119000565>*

The conditions under which sphingolipid- and cholesterol-rich ordered domains form in the plasma membrane of mammalian cells remain unclear. With a few notable exceptions (1, 2), ordered domains remain difficult to directly observe in intact cells. Under many conditions, ordered domains may not even be a constitutive feature of the plasma membrane, but rather one induced in the presence of a stimulus (3, 4). Giant plasma membrane vesicles (GPMVs) represent a natural membrane system in which the domain-forming properties of plasma membrane lipids and proteins can be investigated much more readily than in intact cells (5, 6). They have the advantage over artificial lipid vesicles that they contain a complex natural mixture of lipids and proteins. At low temperatures, the lipids in GPMVs undergo a phase separation in which classical large-scale coexisting liquid-disordered (Ld) and liquid-ordered (Lo) phases form and are easily visualized by light microscopy. These phases have properties very similar to those formed in phase-separating artificial vesicles with simple lipid mixtures in terms of their properties and association with specific proteins. Although large-scale phase separation is only seen in GPMVs at lower temperatures, it has been predicted that nanodomains that decrease in size as temperature increases would persist to much higher temperatures in GPMVs (7). Consistent with this, in some artificial lipid vesicles, nanodomains exist under conditions that large-scale phase separation is not observed, and domain size can decrease as temperature increases (8–10).

Abbreviations: bSM, brain SM; DPBS, Dulbecco's PBS; DPH, 1,6-diphenyl-1,3,5-hexatriene; FAST DiO, 3,3'-dilinoylethoxycarbonyl perchlorate; FRET, Förster resonance energy transfer; GPMV, giant plasma membrane vesicle; Ld, liquid-disordered; Lo, liquid-ordered; M α CD, methyl- α -cyclodextrin; M β CD, methyl- β -cyclodextrin; ODRB, octadecyl rhodamine B; PC, phosphatidylcholine; PFA, paraformaldehyde; POPC, 1-palmitoyl-2-oleoyl-*sn*-glycerol-3-phosphocholine; T end, transition endpoint temperature; T mid, transition midpoint temperature.

¹G. Li and Q. Wang contributed equally to this work.

²To whom correspondence should be addressed.

e-mail: erwin.london@stonybrook.edu

S The online version of this article (available at <https://www.jlr.org>) contains a supplement.

Copyright © 2020 Li et al. Published under exclusive license by The American Society for Biochemistry and Molecular Biology, Inc.

This article is available online at <https://www.jlr.org>

Using GPMVs, studies have shown that modulating the conditions under which cells are grown, modulating cholesterol levels, or adding molecules that can act as anesthetics modulates the stability of ordered domains in GPMVs (11–14). Combined, these studies show that GPMVs are a highly useful system for examining the principles behind lipid domain formation in natural membranes.

In this report, we investigated the relationship between nanodomain and large-scale phase separation in GPMVs and how the formation of both large-scale phases and nanodomains is affected by alteration of plasma membrane lipid composition. We found that ordered nanodomains persist to much higher temperatures than large-scale phase separations. Using methods to modify plasma membrane composition, we found that both large-scale phase separation and nanodomain thermal stability respond to lipid composition in a fashion analogous to what has been previously reported for domain formation in artificial vesicles. However, in some cases, nanodomains responded to a different extent than large-scale phase separations did. Thus, this study provides novel insights into both the inherent ability of plasma membrane lipids to form ordered nanodomains and how the properties of such domains are altered by lipid substitutions in intact cells.

MATERIALS AND METHODS

Materials

Brain SM (bSM), 1-palmitoyl-2-oleoyl-*sn*-glycerol-3-phosphocholine (POPC), cholesterol, and β -hydroxy-5,24-cholestadiene (desmosterol) were purchased from Avanti Polar Lipids (Alabaster, AL). 5-Cholesten-3 α -ol (epicholesterol), 5 β -cholestan-3 β -ol (coprostanol), and 4-cholesten-3-one (cholestenone) were from Steraloids (Newport, RI). 7-Dehydrocholesterol (Fluka brand), lanosterol, 1,6-diphenyl-1,3,5-hexatriene (DPH), and methyl- β -cyclodextrin (M β CD) were from Sigma-Aldrich. Methyl- α -cyclodextrin (M α CD) was purchased from AraChem (Budel, The Netherlands). DMEM medium, MEM α medium, FBS, calf bovine serum, Dulbecco's PBS (DPBS) (200 mg/l KCl, 200 mg/l KH₂PO₄, 8 g/l NaCl, and 2.16 g/l Na₂HPO₄), penicillin and streptomycin, and trypsin with EDTA were from Thermo Fisher Scientific (Waltham, MA). BSA was from Millipore (Kankakee, IL). Octadecyl rhodamine B (ODRB), DTT, 4% (w/v) paraformaldehyde (PFA), and 3,3'-dilinoleoyloxycarbocyanine perchlorate (FAST DiO) were from Invitrogen. Agarose (AMRESCO 0710) was from Cole-Palmer Scientific (Vernon Hills, IL). Glass-bottom four-compartment Cell View cell culture dishes were from Greiner Bio-One (Germany). Microscope slide coverslips (10 \times 10 mm) were from Ted Pella, Inc. (Redding, CA). Lipids were stored at -20°C . PFA and DTT were stored as small aliquots at -20°C to avoid thaw-freeze cycles. Sterol purity was confirmed by TLC as previously (15).

Cell culture

Rat basophilic leukemia (RBL-2H3) cells were a kind gift from Dr. Barbara Baird (Cornell University). Chinese hamster ovary (CCL-61 CHO K-1) cells were obtained from the American Type Culture Collection (Manassas, VA). RBL-2H3 cells were grown in DMEM medium supplemented with 10% FBS (v/v) and 100 U/ml penicillin and streptomycin. CHO cells were grown in MEM α medium with 10% calf bovine serum (v/v). All cells were maintained in a humidified incubator with 5% CO₂ at 37°C.

Lipid/sterol substitution in cultured cells

Cells were seeded 1 day prior to GPMV formation and/or lipid/sterol substitution and were 80–90% confluent the next day. Cells were seeded on 100 mm dishes for Förster resonance energy transfer (FRET) experiments and on 35 mm dishes for microscopy imaging. Lipid-loaded M α CD and sterol-loaded M β CD solutions were prepared and lipid/sterol substitution carried out similarly to (15, 16). Lipid-loaded M α CD and sterol-loaded M β CD solutions were prepared 1 day prior to use. Phospholipids or sterols were dried under nitrogen followed by high vacuum for at least 1 h. They were then hydrated with 40 mM (RBL-2H3) or 50 mM (CHO cells) M α CD for phospholipids or 2.5 mM M β CD for sterols in serum-free medium in a 70°C water bath for 5 min. Concentrations after hydration were 1.5 mM bSM (for RBL-2H3 cells) or 2 mM bSM (for CHO cells), 3 mM POPC, 0.1 mM cholesterol, or 0.4 mM sterol (7-dehydrocholesterol, 4-cholesten-3-one, coprostanol, epicholesterol, desmosterol, lanosterol, or cholesterol). Sterol-loaded M β CD solutions were then sonicated (Cole-Parmer ultrasonic cleaner, Vernon Hills, IL) for 5 min until no visible particles remained. Next, phospholipid-loaded M α CD or sterol-loaded M β CD solutions were incubated at 55°C for 30 min and then at room temperature (for phospholipid-loaded M α CD solutions) or at 37°C (for sterol-loaded M β CD solutions) overnight. M β CD (10 mM) in serum-free medium (cholesterol depletion) was also prepared using the protocol for sterol-loaded M β CD solutions. For lipid/sterol substitution, RBL-2H3 cells were washed twice with 10 ml (100 mm dishes) or 2 ml (35 mm dishes) DPBS, and then 2 ml (100 mm dishes) or 0.5 ml (35 mm dishes) of the prepared phospholipid or sterol-loaded CD solution were added.

The dishes were then incubated at room temperature for 1 h (for phospholipid-loaded M α CD solutions) or at 37°C for 2 h (for sterol-loaded M β CD solutions) while being gently shaken. Next, cells were washed once with DPBS, and 10 ml (100 mm dishes) or 2 ml (35 mm dishes) of complete culture medium were added. Samples were then placed in a 37°C incubator for 2 h recovery. Phospholipid- and sterol-substituted cells were used immediately for GPMV formation.

GPMV formation/isolation

GPMVs were prepared following previous protocols (17). Cells that had been treated as above or untreated controls were used. PFA and DTT were freshly added to 10 mM HEPES, 150 mM NaCl, and 2 mM CaCl₂ (pH 7.4) at a final concentration of 24 mM PFA and (unless otherwise noted) 2 mM DTT. We define this as GPMV buffer. GPMVs were isolated from unsubstituted, lipid-substituted, and sterol-substituted cells. Cells were first washed twice with DPBS and then twice with GPMV buffer lacking PFA and DTT. Next, 2.7 ml (in 100 mm dishes for FRET experiment) or 0.5 ml (in 35 mm dishes for microscopy) of GPMV buffer were added and incubated at 37°C for 2 h, sometimes with gentle shaking. Shaking was found to be necessary for CHO cells. The GPMV-containing supernatant was gently harvested by pipetting, to avoid removal of intact cells, and then centrifuged at 100 *g* for 5 min to remove contaminating cells, which pelleted. The supernatant from this centrifugation was used for the FRET measurements. For microscopy, the supernatant was centrifuged a second time at 500 *g* for 10 min to concentrate the GPMVs. For microscopy imaging, the final GPMV pellet, which was too small to see, plus a small amount of solution (10–20 μ l) above the pellet were resuspended in GPMV buffer. GPMVs were used for FRET or microscopy on the same day as they were prepared.

In experiments to separate larger from smaller GPMVs from RBL-2H3 cells, a second centrifugation was performed at 500 *g* for 10 min. The pellet and supernatant were collected separately. The pellet contained GPMVs that were large enough to see by microscopy. The supernatant contained submicroscopic vesicles.

Lipid concentration in the preparations and vesicle fraction was measured with the DPH assay (see below). About 60–70% of total GPMV lipid was in the submicroscopic fraction. FRET versus temperature was then measured for the total GPMV, large GPMV, and small GPMV fractions as described above.

Estimation of GPMV lipid concentration by DPH

Lipid concentration in GPMVs for FRET experiments was estimated by measurement of DPH fluorescence under conditions in which DPH was in excess (18, 19). A 1 mM lipid stock solution of lipid vesicles containing 1:1 bSM:POPC was prepared to construct a standard curve. To do this, 0.5 μmol of bSM and 0.5 μmol of POPC were mixed and then dried under nitrogen followed by high vacuum for 1 h. Then, the lipids were dissolved in 30 μl of ethanol and then 970 μl of PBS [1 mM KH_2PO_4 , 10 mM Na_2HPO_4 , 137 mM NaCl, and 2.7 mM KCl (pH 7.4)] and incubated at 70°C (in a water bath) for 5 min. Five microliters of 0.2 mM DPH/ethanol were added to either an aliquot from the GPMV stock solution (700 μl to 1 ml) or a range of vesicle aliquots from the 1 mM bSM/POPC vesicle stock solution after dilution to 700 μl to 1 ml with GPMV buffer. After incubation for 5 min at room temperature in the dark, the intensity of DPH fluorescence as a function of lipid concentration was measured at excitation 358 nm and emission 430 nm. Generally, GPMVs from RBL-2H3 cells contained 15–25 μM of lipid and had a volume of about 2.7 ml when isolated from one 100 mm plate. GPMV lipid concentration prepared from CHO cells contained 4–6 μM and had a volume of 2.5 ml when isolated from one 100 mm plate.

Artificial lipid vesicles for FRET experiments

Multilamellar vesicles were prepared containing 1 μmol of lipid (2:1 DOPC:CHOL, 2:1 POPC:CHOL, 1:1:1 bSM:DOPC:CHOL, or 1:1:1 bSM:POPC:CHOL, all mol:mol). The lipids were mixed and then dried under nitrogen followed by high vacuum for 1 h. Then the lipids were dispersed at 70°C (in a water bath) for 5 min in 1 ml of PBS and mixed in a multi-tube vortexer (VWR International) while incubating at 55°C for 15 min. Then, to prepare large unilamellar vesicles from the multilamellar vesicles, the multilamellar vesicles were subjected to seven cycles of freezing using a mixture of dry ice and acetone followed by thawing to about room temperature using warm water, and then were passed through 100 nm polycarbonate filters (Avanti Polar Lipids) 11 times. Samples were diluted to 200 μM with PBS and transferred to 12-well cell culture plates before addition of FRET probes, incubation, and fluorescence was measured as for using GPMVs (see below).

Measurement of the temperature dependence of FRET

FRET measurements were made with DPH as the FRET donor and ODRB as the FRET acceptor. The “F sample” with FRET acceptor was prepared by adding 10 μl from the 500 μM ODRB dissolved in ethanol to 1 ml of GPMVs or lipid vesicles that had been transferred to 12-well Greiner bio-one polystyrene cell culture plates, and after mixing, incubating at 37°C for 1 h in the dark. The “Fo sample” lacking FRET acceptor was also incubated at 37°C for 1 h. [It did not seem to matter whether 10 μl ethanol was added or not (data not shown).] Before fluorescence measurements, DPH (1.8 μl from a 3.4 μM stock solution in ethanol) was added to both the “F sample” and “Fo sample” and incubated at room temperature for 5 min in the dark. Background fluorescence before adding DPH was negligible (<1% of samples containing DPH). To initiate measurements, samples were placed in a cuvette and transferred to a temperature-controlled sample spectrofluorimeter (Horiba PTI Quantmaster) sample holder and cooled to 16°C. DPH fluorescence (excitation 358 nm, emission 430 nm; using 10 nm bandpass slits) was measured increasing temperature at 4°C intervals up to 44°C (for GPMVs)

or 64°C (for lipid vesicles). Between readings, temperature was increased at a rate of 4°C/5 min. The ratio of DPH fluorescence intensity in the presence of ODRB to that in its absence (F/F_0) was then calculated. T end, the measure of the temperature above which segregation of lipids into ordered and disordered domains was fully lost (i.e., the “melting” of ordered domains is complete) was estimated by finding the minimum value of a polynomial fit applied to the F/F_0 using Excel software (Microsoft Corporation, Redmond, WA) and utilities (available at www.wolframalpha.com). [The minimum F/F_0 represents T end because in the absence of domains there is a small decrease in FRET vs. temperature, i.e., F/F_0 increases as temperature is increased (20, 21).]

Control experiments showed that the amount of ODRB bound to GPMVs (as judged by pelleting of GPMVs and GPMV-bound ODRB) was almost identical at 16°C and 40°C, showing that changes in FRET at different temperatures did not reflect changes in ODRB binding to GPMVs (data not shown).

Labeling of GPMVs for microscopy

RBL-2H3 GPMV samples for light microscopy were either labeled before GPMVs were prepared from cells or after GPMVs were isolated from cells. CHO GPMVs were only stained after isolation from cells (because CHO cells were too sensitive to incubate in DPBS). For labeling before GPMV preparation, cells (untreated, phospholipid-substituted, or sterol-substituted) were washed once with DPBS, and after removing the DPBS by aspiration, 5 $\mu\text{g}/\text{ml}$ FAST DiO dye (from a 500 $\mu\text{g}/\text{ml}$ stock solution in ethanol) in 1 ml of DPBS were added to the cells and incubated at 4°C for 10 min. After removal of dye-containing solution by aspiration, the cells were washed five times with DPBS and once with GPMV buffer lacking PFA and DTT. Then, GPMVs were prepared as described above. For labeling after GPMV preparation, 5 $\mu\text{g}/\text{ml}$ FAST DiO or 5 μM ODRB (diluted 100-fold from their stock solutions in ethanol) was added to 100–500 μl of untreated, phospholipid-substituted, or sterol-substituted GPMVs and then incubated at room temperature for 30 min. The labeled GPMVs were pelleted by centrifugation at 500 g for 10 min and, after removal of the supernatant, resuspended in up to 100–500 μl GPMV buffer for microscopy imaging.

GPMV imaging

Seventy microliters of GPMVs were placed in each chamber of a glass-bottom four-compartment Cell View cell culture dish and each chamber was then covered with a 10 mm microscope slide coverslip slightly trimmed to fit in the dish. Each chamber was sealed with agarose (AMRESCO). Chamber temperature was controlled with a CL-100 cooling system (Warner Instrument). An AMG EVOS fluorescence microscope (Thermo Fisher Scientific) was used to image GPMVs. Images of GPMVs were taken over a range of 2–30°C at intervals of 4°C and incubating for 5 min after the sample reached the desired temperature prior to taking pictures. Microscopy was performed the same day that GPMVs were prepared, although no difference was seen when GPMVs were stored for up to 2 days at 4°C (data not shown). For each experiment, at the temperatures at which some but not all GPMVs had domains, the domain status of 50 GPMVs was measured for three separate fields. The results shown are for three independent experiments, unless otherwise noted. To define the transition from temperatures at which domains form to those at which they do not form, the fraction of GPMVs with domains was measured as a function of temperature, fitted to a sigmoidal curve (Slidewrite; Advanced Graphics Software, Encinitas, CA), and then T mid, the value at which 50% of the GPMVs contained domains, and T end, which was defined as the point at which <1% of the GPMVs contained domains, were calculated.

TLC analysis of GPMV lipids

Unsubstituted, lipid-substituted, or sterol-substituted GPMVs were concentrated by centrifugation at 20,000 *g* at 4°C for 30 min, and then the lipids in the pellet (about 80% yield of total lipid) were extracted by adding 3:2 (v:v) hexanes:isopropanol. The organic solvent was dried under N₂ gas and lipids were dissolved in 1:1 chloroform:methanol for loading onto TLC plates. Lipids were chromatographed in 54:18:18 (v:v) chloroform/methanol/acetic acid and detected as described previously (16).

RESULTS

Assays for domain formation

Coexisting large Lo and Ld domains/phases in GPMVs can be visualized by light microscopy. Large Ld domains can be detected as regions enriched in a fluorescence probe that partitions favorably into Ld domains, while Lo domains appear depleted in that type of fluorescent probe. GPMVs are heterogeneous, and the parameter conventionally used to estimate domain levels is the fraction of GPMVs containing coexisting ordered and disordered domains (22). When temperature is increased, the fraction of GPMVs with domains large enough to visualize decreases from near 100% to 0%. A transition midpoint temperature (T mid or T misc) was defined as the temperature at which 50% of GPMVs show coexisting ordered and disordered domains (22). The transition endpoint (T end) was defined as the temperature above which <1% of GPMVs contained ordered domains.

To detect nanodomains in GPMVs, FRET was used. A FRET assay developed to detect ordered domains in bacteria (1), using TMADPH as donor and ODRB as acceptor, was adapted to use in GPMVs with DPH. In membranes with coexisting ordered and disordered domains, there is partial segregation of DPH [which tends to equally partition between ordered and disordered domains (23)] from ODRB [which localizes preferentially in disordered domains (24)]. As a result, the fraction of DPH fluorescence unquenched by the FRET acceptor, which equals the ratio of DPH fluorescence in the presence of ODRB to that in the absence of ODRB (F/F_o), is elevated relative to F/F_o in membranes fully in the Ld state. (The fraction of FRET equals the fraction of fluorescence quenched, $1-F/F_o$.) Samples with coexisting domains at lower temperatures generally show a marked decrease in F/F_o at elevated temperatures. The reason is that the average distance between DPH and ODRB decreases when Lo domains disappear as they melt/mix with Ld lipids at elevated temperatures. (Because Lo domains are ordered, we refer to the order to disorder transition associated with miscibility at high temperature as a melting transition.)

To confirm the ability of this assay to detect ordered domain formation, FRET was measured in artificial lipid vesicles containing mixtures of SM, phosphatidylcholine (PC), and cholesterol known to form coexisting Lo and Ld domains (25, 26) (supplemental Fig. S1; diamonds, squares). As expected in such samples, F/F_o was elevated at low temperatures and decreased at elevated temperatures. In the

control Ld state vesicles in which lipids were homogeneously mixed, F/F_o was largely temperature independent (supplemental Fig. S1; triangles, circles).

Phase separation and nanodomain formation in GPMVs from RBL-2H3 cells

GPMVs were prepared from RBL-2H3 cells using the DTT/PFA protocol and domain formation examined by microscopy and FRET. In agreement with prior studies (22), Fig. 1A and the examples of GPMVs in supplemental Fig. S2 show that GPMVs formed coexisting large Lo and Ld phases at low temperatures, and these phases disappeared as temperature was increased. Both T mid and T end increased as the concentration of DTT used to prepare the GPMVs was increased, again in agreement with previous studies (22). The T mid was as high as 19°C, and the T end was as high as 25°C when GPMVs were prepared with 5 mM DTT (Table 1). At the widely used concentration of 2 mM DTT, the T mid was 15°C and the T end was 23°C. These values are close to those reported previously (22).

FRET showed behavior similar to that measured by microscopy in the sense that higher DTT levels resulted in increased formation and increased thermal stability of ordered domains as measured by T end (Fig. 1B, Table 1). (FRET curves were too incomplete to estimate T mid.) T end measured by FRET was much higher than that detected by microscopy, as high as 38°C with 2–5 mM DTT. This shows that nanodomains persist to much higher temperatures than large-scale phase separation.

Control experiments showed that the difference between domain stability by microscopy and FRET did not reflect use of different fluorescent probes in the two methods. When ODRB was used in microscopy experiments to stain Ld domains, large-scale phase separation appeared to be,

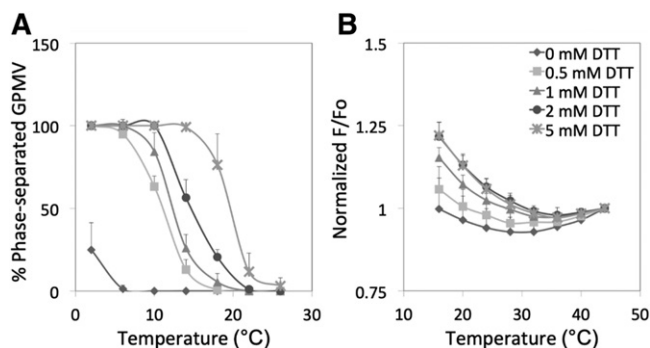


Fig. 1. Temperature dependence of phase separation and nanodomain formation in RBL-2H3 GPMVs: effect of DTT concentration. A: Phase separation assayed by fluorescence microscopy. B: Nanodomain formation assayed by FRET. Samples for microscopy contained FAST DiO. Samples for FRET contained DPH and ODRB. GPMVs prepared with DTT and 24 mM PFA. F/F_o values are normalized to 1 at the highest temperature at which measurements were made (44°C). Unnormalized F/F_o values at 44°C for this and later figures are shown in supplemental Table S1. Symbols: no DTT (diamonds); 0.5 mM DTT (squares); 1 mM DTT (triangles); 2 mM DTT (circles); 5 mM DTT (crosses). In this and the following figures, mean values and standard deviations (up bars only) for $n = 3$ are shown unless otherwise noted.

TABLE 1. T mid and T end values for large-scale phase separation and nanodomain formation for RBL-2H3 GPMVs prepared with 24 mM at different DTT concentrations

DTT Concentration (mM)	Phase Separation		Nanodomains
	T mid	T end	T end
0	0.5 ± 2.0	5.4 ± 2.4	26.7 ± 2.1
0.5	10.6 ± 2.5	15.1 ± 3.9	31.4 ± 2.5
1	12.5 ± 2.0	19.2 ± 3.6	34.6 ± 1.4
2	14.8 ± 0.7	22.7 ± 0.4	38.2 ± 1.1
5	19.1 ± 0.9	24.7 ± 5.0	37.4 ± 1.5

The data were fitted to a sigmoidal curve of percent GPMVs with domains versus temperature, assuming the limit at extremely low temperature would equal 100% of vesicles containing domains. For phase separation, T mid was defined as temperature at which 50% of the vesicles would have domains, and T end the temperature above which less than 1% of vesicles contain domains. For nanodomains, T end was defined as the temperature at which F/F₀ was a minimum (see Methods). Mean values and standard deviations from the results from three preparations are shown.

if anything, slightly less thermally stable than when detected by FAST DiO (supplemental Fig. S3A). It should be noted that, under some conditions, illumination can induce large domain formation (27), but the large-scale phase separations observed were present as soon as the samples were visualized, indicating that illumination was not a factor in their formation.

We found that the GPMV preparations contained some submicroscopic vesicles. FRET values for entire GPMV preparations and submicroscopic vesicles in the GPMV preparations were very similar to those for the (more easily pelleted) large GPMVs (supplemental Fig. S3B). This shows that the difference between T end by microscopy and FRET did not reflect a difference in physical properties of larger and smaller vesicles.

The formation of both large-scale phase separation and nanodomains in these samples involved an equilibrium process. For phase separation, this was shown by the observation that changes in domain formation were reversible upon cooling and upon reheating. However, the transition temperature decreased a few degrees during cooling and during a second reheating step (supplemental Fig. S3C). The transition temperature was also not affected significantly if samples were visualized up to at least 2 days after GPMVs were prepared (data not shown). FRET changes versus temperature were also reversible, a repeat scan being almost superimposable with the original temperature scans, although a small decrease in thermal stability might have occurred after one round of heating and cooling (supplemental Fig. S3D).

Effect of altering phospholipid/sphingolipid composition upon domain stability

In previous studies (16, 19), we used cyclodextrins (CDs) to manipulate plasma membrane phospholipid and sphingolipid composition in a fashion that should stabilize or destabilize domain formation (as predicted by the effect of lipid composition upon domain formation in artificial vesicles). To investigate whether changing lipids in cells affects plasma membrane domain formation, GPMVs were prepared from RBL-2H3 cells in which phospholipid composition had been altered by incubation with M α CD/lipid mixtures under conditions that resulted in nearly complete replacement of endogenous outer leaflet phospholipid and SM with exogenous lipid (16, 19). [M α CD does not carry sterols, and

so does not perturb cell sterol content (28).] **Figure 2A** and **Table 2** show that replacement of plasma membrane outer leaflet lipids with SM prior to GPMV preparation stabilized large-scale ordered domain formation in GPMVs, while substitution with the unsaturated lipid, POPC, destabilized it, as predicted from the effect of these lipids upon domain formation in artificial lipid vesicles. These results are consistent with previous studies showing that the stability of large-scale domain formation in GPMVs from cells grown at different temperatures is modulated in a fashion that likely reflects changes in lipid composition (13). Analogous effects of lipid substitution on nanodomain formation were observed by FRET (Fig. 2B, Table 2). TLC of the lipids of GPMVs prepared from cells before and after phospholipid/sphingolipid exchange confirmed that the PC/SM ratio was altered as expected (supplemental Fig. S4). Omitting the 2 h recovery step in complete serum-containing medium after the lipid exchange using M α CD/lipid mixtures did not greatly affect large-scale domain formation (supplemental Fig. S5). This indicates that the changes in domain-forming properties after exchange are stable for hours after the exchange step. This is not a surprise, as these types of changes in lipid composition reverse only slowly after lipid exchange (16, 19).

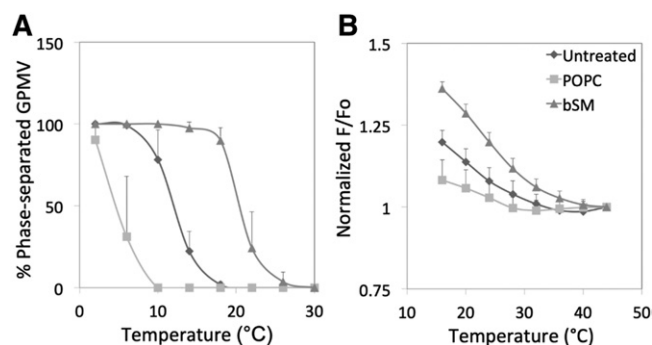


Fig. 2. Effect of phospholipid exchange in cells upon phase separation and nanodomain formation in RBL-2H3 GPMVs. A: Phase separation assayed by fluorescence microscopy. B: Nanodomain formation assayed by FRET. F/F₀ values are normalized to a value of 1 at the highest temperature at which measurements were made. Symbols: untreated (diamonds); after exchange with POPC (squares); after exchange with bSM (triangles). Samples prepared using 2 mM DTT and 24 mM PFA.

TABLE 2. T mid and T end values for large-scale phase separation and nanodomain formation for RBL-2H3 GPMVs prepared using 2 mM DTT and 24 mM PFA after different substitutions or additions

Substitution	Phase Separation		Nanodomains
	T mid	T end	T end
Untreated	12.2 ± 1.3	18.6 ± 2.1	38.5 ± 2.4
POPC	4.4 ± 1.9	7.6 ± 1.6	33.3 ± 2.1
SM	20.1 ± 1.3	25.9 ± 2.4	42.5 ± 1.1
Coprostanol	2.6 ± 1.1	7.6 ± 3.3	32.9 ± 2.1
4-Cholesten-3-one	-1.3 ± 0.8	11.1 ± 1.1	32.9 ± 2.7
Desmosterol	10.1 ± 1.5	14.9 ± 2.1	37.1 ± 3.5
Epicholesterol	10.9 ± 1.5	18.0 ± 2.7	31.4 ± 0.2
Lanosterol	11.5 ± 1.8	18.5 ± 3.9	34.5 ± 1.8
7-Dehydrocholesterol	21.9 ± 1.5	25.7 ± 1.8	44.1 ± 2.9
Cholesterol depleted	2.9 ± 2.5	17.8 ± 1.8	30.3 ± 1.4
Cholesterol loaded (0.1 mM)	16.8 ± 1.2	20.5 ± 3.6	37.1 ± 1.3
Cholesterol loaded (0.4 mM)	19.7 ± 2.8	24.1 ± 2.4	38.8 ± 2.2

Mean values and standard deviations from the results from three preparations are shown, except for untreated samples (samples without any lipid substitutions) for which n = 9.

Effect of altering sterol composition upon domain stability

Experiments were also carried out to determine whether sterol (or steroid if the molecule lacks a OH group) substitution altered GPMV ordered domain formation in a fashion similar to which it affects ordered domain formation in artificial lipid vesicles. Previous studies by our group (20, 22, 29–31) and others (32, 33) have shown that sterols can stabilize or destabilize ordered domain formation in artificial vesicles depending on sterol structure. Sterol substitution in cells using sterols with a range of domain-stabilizing or -destabilizing properties has been used in many studies to determine whether membrane domain formation influences a biological process (15, 34). Sterol substitution was carried out as previously (15), treating RBL-2H3 cells with sterol-loaded M β CD at cyclodextrin concentrations too low to bind phospholipid (35). We previously found that this leads to efficient replacement of endogenous cholesterol with exogenous sterol (15). GPMVs were prepared from the sterol-substituted RBL-2H3 cells. **Figure 3A** and C and Table 2 show that sterol substitution altered the thermal stability of large-scale phase formation. Relative to untreated cells, the largest reductions in large-scale domain stability were observed with 4-cholesten-3-one and coprostanol, previously shown to strongly inhibit ordered domain formation (20, 29). Substitution with most other sterols tested (desmosterol, lanosterol, and epicholesterol) or simple depletion of cholesterol decreased the thermal stability of large-scale domain formation to a moderate degree. Exchange using cholesterol-loaded M β CD, which can increase cholesterol membrane concentration (15), or with 7-dehydrocholesterol stabilized large-scale domain formation. It should be noted that the effects of increasing or decreasing cholesterol levels in GPMVs upon large-scale phase separation are in agreement with previous studies (11, 12).

The effect of sterol substitutions upon nanodomain formation was also examined (Fig. 3B, D; Table 2). The pattern observed for the various sterols was similar to that for large-scale domain formation, but also showed some important differences. Unlike what was observed for phase separation, epicholesterol destabilized nanodomain formation much more than lanosterol and desmosterol, and to an extent similar to the destabilization observed with

cholestenone and coprostanol. Also, cholesterol replacement restored T end to values similar to those before cholesterol depletion, but did not stabilize nanodomain formation relative to GPMVs from untreated cells, unlike its effect upon T end for large-scale phase separation. It should be noted that differences between the lipid-dependence of nanodomain formation and large-scale phase separation can also be seen in artificial lipid vesicles in which different sterols have been incorporated (29, 30, 33). Interestingly, the order of sterol substitution effects on nanodomain stability (but not phase separation) is very close to that observed for these sterols when FRET-detected ordered domain stability is measured in asymmetric artificial lipid vesicles (20), and to the order in which these sterols support endocytosis (15).

GPMVs from CHO cells show similar stability patterns as those from RBL-2H3 cells

To determine whether GPMV properties and response to lipid changes were specific to RBL-2H3 cells, some experiments were repeated in CHO cells. Large phases (**Fig. 4A**) and nanodomains (Fig. 4B) were also observed in GPMVs prepared from CHO cells. They were slightly more thermally stable than those formed by RBL-2H3 cells (Fig. 2A). The effect of lipid substitution upon the stability of nanodomain formation was also examined in CHO cells (Fig. 4B), and again nanodomain stability was slightly greater than in RBL-2H3 cells. In addition, substitution affected both large-scale phase separation and ordered nanodomain formation as expected, with decreased stability upon substitution with POPC and increased stability upon substitution with SM. Note that the apparent T end for CHO cell GPMVs appears to be a bit higher than that for RBL-2H3 cells (compare Figs. 2 and 4). This is consistent with the higher fraction of SM relative to PC in CHO cells relative to RBL-2H3 cells (supplemental Fig. S4C).

Relationship between large-scale and nanodomain transition temperatures

Figure 5 illustrates the relationship between T end for large-scale phase formation and nanodomain formation in RBL-2H3 cells under the various experimental conditions studied here. There is a significant correlation between

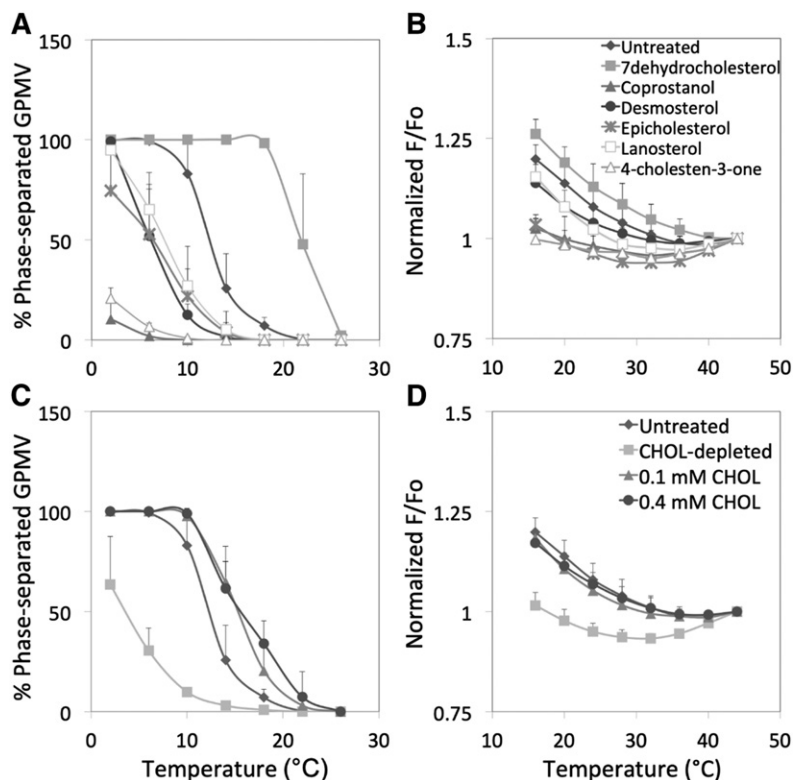


Fig. 3. Effect of sterol exchange in cells upon phase separation and nanodomain formation in RBL-2H3 GPMVs. A, C: Phase separation assayed by fluorescence microscopy. Symbols: untreated (diamonds); 7-dehydrocholesterol (filled squares); coprostanol (filled triangles); desmosterol (circles); epicholesterol (crosses); lanosterol (open squares); 4-cholesten-3-one (open triangles). B, D: Nanodomain formation assayed by FRET. Symbols: untreated (diamonds); cholesterol-depleted (filled squares); exchange with 0.1 mM cholesterol (filled triangles); exchange with 0.4 mM cholesterol (circles). Samples prepared using 2 mM DTT and 24 mM PFA ($n = 3$; except $n = 9-10$ for the untreated samples).

T end values for phase and nanodomain stability ($r^2 = 0.60$) with T end being between about 15°C and 25°C higher for nanodomains than for large-scale domain formation. The lipid dependence of the difference between these parameters suggests that although the two parameters are related, they sometimes respond differently to changes in lipid structure.

DISCUSSION

Nanodomain and large domain formation and properties in GPMVs

The primary conclusions of this report are that: 1) ordered lipid nanodomains are present in GPMVs at temperatures well above those in which there is large-scale phase separation; 2) alteration of plasma membrane lipid composition and properties in intact cells results in corresponding changes in the composition and properties of the GPMVs; and 3) altering GPMV lipid composition sometimes alters nanodomain thermal stability differently than that of large phase separation.

Effect of lipid substitution upon nanodomain formation

Changing plasma membrane lipid composition affected the thermal stability of ordered domains in GPMVs prepared from cells subjected to lipid exchange. The changes in stability as a function of lipid composition were similar to the effect of the same changes in lipid composition upon the stability of ordered domains in asymmetric artificial lipid vesicles (21). In addition, sterols found to stabilize or destabilize ordered domain formation in asymmetric lipid

vesicles had the analogous effect upon ordered nanodomain stability in GPMVs (20).

In this regard, it is noteworthy that the effect of sterol structure upon nanodomains matches the pattern for the effect of sterol structure upon endocytosis (15). One caveat is that there can be differences in the extent of exchange for different sterols (15), which complicates quantitative comparison of the extent of altered stability in GPMVs to that of artificial vesicles with well-defined compositions. Nevertheless, the overall pattern shows that the physical principles controlling ordered domain formation by lipids in simple bilayers (at least when they have asymmetry mimicking that in cells) are likely to apply to the more compositionally complex lipid bilayers in natural membranes.

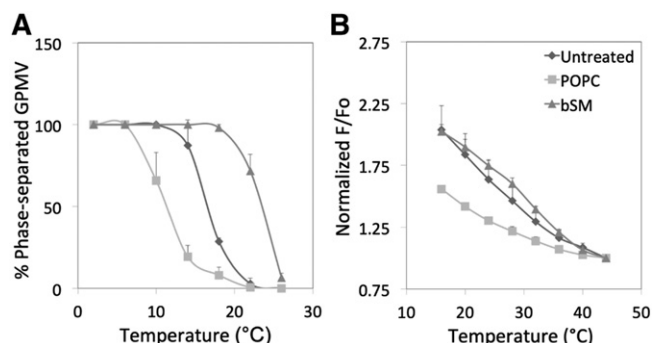


Fig. 4. Temperature dependence of and effect of phospholipid exchange upon phase separation and nanodomain formation in CHO cells. A: Phase separation assayed by fluorescence microscopy. B: Nanodomain formation assayed by FRET. Symbols: untreated (diamonds); after exchange with POPC (squares); after exchange with bSM (triangles). Samples prepared using 2 mM DTT and 24 mM PFA.

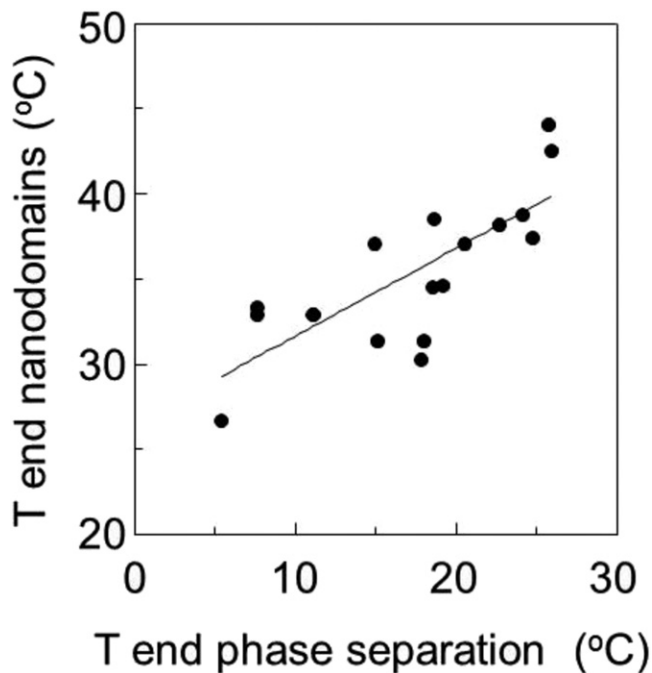


Fig. 5. Correlation between T_{end} for large-scale phase separation and T_{end} for nanodomain formation for RBL-2H3 GPMVs. Data are from Tables 1 and 2 ($r^2 = 0.60$).

Nanodomain formation and stability in GPMVs

The observation that nanodomains, here meaning regions of distinct lipid composition and/or properties that are in the nanometer size range, can exist under conditions in which large-scale domains are not stable is consistent with the behavior of lipids in artificial lipid vesicles. Conditions under which nanoscale domains form but there is no large-scale phase separation have been reported for a number of lipid mixtures (8–10). The reasons that nanodomains might not merge into larger domains has been much discussed in the literature, although no consensus has been reached (9, 36–38). It has been proposed that whatever factor opposes the merger of nanodomains becomes predominant when line tension between L_o and L_d domains falls below 0.3 pN (9, 37).

It has also been found by FRET that some (but not all) lipid mixtures show a relatively gradual temperature-dependent decrease in ordered domain size as temperature is increased (8). A decrease in domain size as temperature is increased has also been observed as a lipid mixture approaches a critical point, and it has been proposed that transient submicroscopic domains exist above the critical point, including the case of GPMVs (7, 36). The prediction for the temperature dependence of domain size above the critical point temperature is in good agreement with our experimental results. It has been proposed that domains of 22 nm size would be present at 37°C in GPMVs, 14°C higher than the critical temperature, which would be close to T_{mid} . The slightly higher values observed for the persistence of nanodomains above the critical temperature (15–25°C) may reflect the ability of FRET to detect domains smaller than 22 nm in size. Roughly speaking, FRET can

detect domains larger than the critical interaction distance for FRET, R_o , for the FRET donor-acceptor pair being used, about 4 nm for the FRET probes used in this report (8).


It should be noted that if large-scale phases collapse and are replaced by nanodomains whenever line tension at domain boundaries drops below a critical value, then nanodomains could exist for different reasons in membranes with different lipid compositions. In the case of membranes that are approaching the critical point temperature, ordered and disordered domain compositions and properties approach each other, and thus line tension at domain boundaries may fall below the value allowing large-scale phases to form. Thus, nanodomains might form before the critical point temperature is reached. In other words, whereas some lipid mixtures may have low line tensions at domain boundaries over a wide range of compositions, others may only have low line tensions at domain boundaries near critical points.

Biological implications

The observation that as temperature is increased large-scale domain formation disappears in GPMVs well before nanodomains suggests that in biological membranes nanodomains are more likely to form than large-scale domains. The observation that altering lipids in intact cells by exchange not only alters GPMV lipid composition, but also GPMV properties, shows that when plasma membrane lipid composition is modulated by exchange, the capacity of the plasma membrane to form domains is also likely to be modulated. Even in the absence of detailed measurement of lipid composition changes, the extent to which nanodomains are altered in GPMVs by lipid exchange should be a useful measure of the extent to which the capacity to form domains in intact cells is altered by lipid substitution. Extrapolating from the effect of lipid composition upon large-scale phase separation to lipid behavior in cells may be less accurate, because some of the more biologically relevant lipid compositions can form nanodomains but lack the capacity to form large-scale phase separations, even in artificial lipid vesicles (10). Presumably, some factors that influence the ability of nanodomains to form differ from the factors that allow nanodomains to merge into larger domains.

In addition, the results of this study also show that the change in both plasma membrane composition and behavior persists for hours after the lipid exchange step. This means that experiments on plasma membranes carried out hours after a lipid substitution step should still reflect the effects of the lipid substitution. This should enhance the utility of lipid exchange as a method to probe the functions of membrane domains *in vivo*.

On the other hand, in view of the highly perturbed structure of GPMVs, it must be kept in mind that the fact that nanodomains persisted to physiological temperature in these studies does not mean that they are present in intact cells. This perturbation includes changes in the lipid asymmetry found in plasma membranes. At present, it is known that at least some of the asymmetry of phosphatidylserine is lost in GPMVs (39). In addition, it is not clear if GPMV

lipids represent a biased subset of plasma membrane lipids. Experiments using milder methods to prepare GPMVs and experiments in intact cells will be needed to further investigate these issues. 

REFERENCES

- LaRocca, T. J., P. Pathak, S. Chiantia, A. Toledo, J. R. Silvius, J. L. Benach, and E. London. 2013. Proving lipid rafts exist: membrane domains in the prokaryote *Borrelia burgdorferi* have the same properties as eukaryotic lipid rafts. *PLoS Pathog.* **9**: e1003353.
- Toulmay, A., and W. A. Prinz. 2013. Direct imaging reveals stable, micrometer-scale lipid domains that segregate proteins in live cells. *J. Cell Biol.* **202**: 35–44.
- Sohn, H. W., P. Tolar, and S. K. Pierce. 2008. Membrane heterogeneities in the formation of B cell receptor-Lyn kinase microclusters and the immune synapse. *J. Cell Biol.* **182**: 367–379.
- Holowka, D., and B. Baird. 2016. Roles for lipid heterogeneity in immunoreceptor signaling. *Biochim. Biophys. Acta.* **1861**: 830–836.
- Sengupta, P., A. Hammond, D. Holowka, and B. Baird. 2008. Structural determinants for partitioning of lipids and proteins between coexisting fluid phases in giant plasma membrane vesicles. *Biochim. Biophys. Acta.* **1778**: 20–32.
- Baumgart, T., A. T. Hammond, P. Sengupta, S. T. Hess, D. A. Holowka, B. A. Baird, and W. W. Webb. 2007. Large-scale fluid/fluid phase separation of proteins and lipids in giant plasma membrane vesicles. *Proc. Natl. Acad. Sci. USA.* **104**: 3165–3170.
- Veatch, S. L., P. Cicuta, P. Sengupta, A. Honerkamp-Smith, D. Holowka, and B. Baird. 2008. Critical fluctuations in plasma membrane vesicles. *ACS Chem. Biol.* **3**: 287–293.
- Pathak, P., and E. London. 2011. Measurement of lipid nanodomain (raft) formation and size in sphingomyelin/POPC/cholesterol vesicles shows TX-100 and transmembrane helices increase domain size by coalescing preexisting nanodomains but do not induce domain formation. *Biophys. J.* **101**: 2417–2425.
- Tsai, W. C., and G. W. Feigenson. 2019. Lowering line tension with high cholesterol content induces a transition from macroscopic to nanoscopic phase domains in model biomembranes. *Biochim. Biophys. Acta Biomembr.* **1861**: 478–485.
- Konyakhina, T. M., S. L. Goh, J. Amazon, F. A. Heberle, J. Wu, and G. W. Feigenson. 2011. Control of a nanoscopic-to-macroscopic transition: modulated phases in four-component DSPC/DOPC/POPC/Chol giant unilamellar vesicles. *Biophys. J.* **101**: L8–L10.
- Levental, I., F. J. Byfield, P. Chowdhury, F. Gai, T. Baumgart, and P. A. Janmey. 2009. Cholesterol-dependent phase separation in cell-derived giant plasma-membrane vesicles. *Biochem. J.* **424**: 163–167.
- Zhao, J., J. Wu, and S. L. Veatch. 2013. Adhesion stabilizes robust lipid heterogeneity in supercritical membranes at physiological temperature. *Biophys. J.* **104**: 825–834.
- Burns, M., K. Wisser, J. Wu, I. Levental, and S. L. Veatch. 2017. Miscibility transition temperature scales with growth temperature in a zebrafish cell line. *Biophys. J.* **113**: 1212–1222.
- Gray, E., J. Karstake, B. B. Machta, and S. L. Veatch. 2013. Liquid general anesthetics lower critical temperatures in plasma membrane vesicles. *Biophys. J.* **105**: 2751–2759.
- Kim, J. H., A. Singh, M. Del Poeta, D. A. Brown, and E. London. 2017. The effect of sterol structure upon clathrin-mediated and clathrin-independent endocytosis. *J. Cell Sci.* **130**: 2682–2695.
- Li, G., J. Kim, Z. Huang, J. R. St Clair, D. A. Brown, and E. London. 2016. Efficient replacement of plasma membrane outer leaflet phospholipids and sphingolipids in cells with exogenous lipids. *Proc. Natl. Acad. Sci. USA.* **113**: 14025–14030.
- Sezgin, E., H. J. Kaiser, T. Baumgart, P. Schwillie, K. Simons, and I. Levental. 2012. Elucidating membrane structure and protein behavior using giant plasma membrane vesicles. *Nat. Protoc.* **7**: 1042–1051.
- London, E., and G. W. Feigenson. 1978. A convenient and sensitive fluorescence assay for phospholipid vesicles using diphenylhexatriene. *Anal. Biochem.* **88**: 203–211.
- Li, G., S. Kakuda, P. Suresh, D. Canals, S. Salamone, and E. London. 2019. Replacing plasma membrane outer leaflet lipids with exogenous lipid without damaging membrane integrity. *PLoS One.* **14**: e0223572.
- St Clair, J. W., and E. London. 2019. Effect of sterol structure on ordered membrane domain (raft) stability in symmetric and asymmetric vesicles. *Biochim. Biophys. Acta Biomembr.* **1861**: 1112–1122.
- Wang, Q., and E. London. 2018. Lipid structure and composition control consequences of interleaflet coupling in asymmetric vesicles. *Biophys. J.* **115**: 664–678.
- Levental, I., M. Grzybek, and K. Simons. 2011. Raft domains of variable properties and compositions in plasma membrane vesicles. *Proc. Natl. Acad. Sci. USA.* **108**: 11411–11416.
- Lentz, B. R., Y. Barenholz, and T. E. Thompson. 1976. Fluorescence depolarization studies of phase transitions and fluidity in phospholipid bilayers. 2 Two-component phosphatidylcholine liposomes. *Biochemistry.* **15**: 4529–4537.
- Loura, L. M., A. Fedorov, and M. Prieto. 2001. Exclusion of a cholesterol analog from the cholesterol-rich phase in model membranes. *Biochim. Biophys. Acta.* **1511**: 236–243.
- Pathak, P., and E. London. 2015. The effect of membrane lipid composition on the formation of lipid ultrananodomains. *Biophys. J.* **109**: 1630–1638.
- Petruzielo, R. S., F. A. Heberle, P. Drazba, J. Katsaras, and G. W. Feigenson. 2013. Phase behavior and domain size in sphingomyelin-containing lipid bilayers. *Biochim. Biophys. Acta.* **1828**: 1302–1313.
- Morales-Pennington, N. F., J. Wu, E. R. Farkas, S. L. Goh, T. M. Konyakhina, J. Y. Zheng, W. W. Webb, and G. W. Feigenson. 2010. GUV preparation and imaging: minimizing artifacts. *Biochim. Biophys. Acta.* **1798**: 1324–1332.
- Lin, Q., and E. London. 2014. Preparation of artificial plasma membrane mimicking vesicles with lipid asymmetry. *PLoS One.* **9**: e87903.
- Xu, X., and E. London. 2000. The effect of sterol structure on membrane lipid domains reveals how cholesterol can induce lipid domain formation. *Biochemistry.* **39**: 843–849.
- Xu, X., R. Bittman, G. Dupontail, D. Heissler, C. Vilcheze, and E. London. 2001. Effect of the structure of natural sterols and sphingolipids on the formation of ordered sphingolipid/sterol domains (rafts) Comparison of cholesterol to plant, fungal, and disease-associated sterols and comparison of sphingomyelin, cerebrosides, and ceramide. *J. Biol. Chem.* **276**: 33540–33546.
- Wang, J., Megha, and E. London. 2004. Relationship between sterol/steroid structure and participation in ordered lipid domains (lipid rafts): implications for lipid raft structure and function. *Biochemistry.* **43**: 1010–1018.
- Wenz, J. J., and F. J. Barrantes. 2003. Steroid structural requirements for stabilizing or disrupting lipid domains. *Biochemistry.* **42**: 14267–14276.
- Beattie, M. E., S. L. Veatch, B. L. Stottrup, and S. L. Keller. 2005. Sterol structure determines miscibility versus melting transitions in lipid vesicles. *Biophys. J.* **89**: 1760–1768.
- Kim, J., and E. London. 2015. Using sterol substitution to probe the role of membrane domains in membrane functions. *Lipids.* **50**: 721–734.
- Anderson, T. G., A. Tan, P. Ganz, and J. Seelig. 2004. Calorimetric measurement of phospholipid interaction with methyl-beta-cyclodextrin. *Biochemistry.* **43**: 2251–2261.
- Honerkamp-Smith, A. R., P. Cicuta, M. D. Collins, S. L. Veatch, M. den Nijs, M. Schick, and S. L. Keller. 2008. Line tensions, correlation lengths, and critical exponents in lipid membranes near critical points. *Biophys. J.* **95**: 236–246.
- Usery, R. D., T. A. Enoki, S. P. Wickramasinghe, M. D. Weiner, W. C. Tsai, M. B. Kim, S. Wang, T. L. Torng, D. G. Ackerman, F. A. Heberle, et al. 2017. Line tension controls liquid-disordered + liquid-ordered domain size transition in lipid bilayers. *Biophys. J.* **112**: 1431–1443.
- Schick, M. 2018. Strongly correlated rafts in both leaves of an asymmetric bilayer. *J. Phys. Chem. B.* **122**: 3251–3258.
- Keller, H., M. Lorizate, and P. Schwillie. 2009. PI(4,5)P2 degradation promotes the formation of cytoskeleton-free model membrane systems. *ChemPhysChem.* **10**: 2805–2812.